

# Syndrome Measurement Strategies for the $[[7,1,3]]$ Code

Yaakov S. Weinstein<sup>1</sup>

<sup>1</sup>*Quantum Information Science Group, MITRE, 200 Forrester Rd, Princeton, NJ 08540, USA*

Quantum error correction requires the measurement of error syndromes to properly locate and identify errors. Here we compare three syndrome measurement strategies for the  $[[7,1,3]]$  quantum error correction code: Shor states, Steane states, and one ancilla qubit. The first two of these strategies are fault tolerant while the third is not. For each strategy we compare the fidelities of applying 50 logical gates with quantum error correction applied at different intervals. We then compare the fidelities for the different syndrome measurement strategies. Our simulations show that the optimal syndrome measurement strategy depends on the details of the error environment. The simulations thus allow a quantum computer programmer to weigh computational accuracy versus resource consumption for a particular error environment. In addition, we show that applying syndrome measurement that are unnecessary from the standpoint of quantum fault tolerance may be helpful in achieving better accuracy or in lowering resource consumption. Finally, our simulations show that the non-fault tolerant syndrome measurement strategy gives comparable accuracy results with those that are fault tolerant.

PACS numbers: 03.67.Pp, 03.67.-a, 03.67.Lx

## I. INTRODUCTION

Quantum error correction (QEC) codes can be used to make quantum information robust against errors [1–3]. This is done by encoding some number of logical qubits into a larger number of physical qubits. Syndrome measurements, parity measurements between multiple qubits, are then used to determine the presence and location of an error and a recovery operation may be applied to correct the error.

A paradigmatic example of a QEC code is the Steane  $[[7,1,3]]$  code [4] in which one logical qubit is encoded into 7 physical qubits. The encoding is robust against all single (physical) qubit errors. In the initial formulation of the code 6 syndrome measurements were needed to detect and identify an error: 3 for bit-flip errors, and 3 for phase-flip errors each requiring one ancilla qubit as shown in Fig. 1.

QEC thus allows for the storage of quantum information. However, for successful quantum computation storage alone is insufficient. Quantum information must be manipulated so as to perform quantum operations such as gates and measurements. These processes must be performed in such a way so as keep the quantum infor-

mation protected from error. In addition, we would like to ensure that if an error does occur to a (physical) qubit it cannot spread to multiple additional qubits. All of this can be done by following the strictures of quantum fault tolerance (QFT) [5–8]. QFT allows for successful quantum computation despite the possibility of error in the basic quantum operations.

Through the lens of QFT, the syndrome measurement scheme of Fig. 1 is flawed because errors on one qubit can spread uncontrollably throughout the circuit. For example, an error to one of the ancilla qubits used for the syndrome measurement can easily effect the four ‘data’ qubits it interacts with and from there spread to even more qubits. To make syndrome measurement adhere to the rules of QFT any ancilla qubit should interact with only one data qubit. There are a number of schemes that allow this to be done for the  $[[7,1,3]]$  QEC code. In this paper we will look at two of those schemes and compare, via fidelity, their performance to the non-fault tolerant scheme in which only one qubit is used for each syndrome measurement. This will be done via numerical simulations of a sequence of 50 encoded quantum gates. In addition, we will apply QEC at different intervals during the 50 gates to determine how often QEC should be applied for the different syndrome measurement schemes. All of the simulations will be done in a noisy environment.

One method of performing the  $[[7,1,3]]$  code syndrome measurements in a fault tolerant fashion is to substitute each single qubit of Fig. 1 with a four-qubit Shor state [6]. Shor states are GHZ states with Hadamard gates appended to each qubit. The Shor state construction is made fault tolerant by applying appropriate verifications [30]. The parity of the measurements of the Shor state qubits is the outcome of the syndrome measurement. This process is shown in Fig. 2. To ensure there are no errors during the syndrome measurement a single application of fault tolerant QEC requires that the entire set of syndrome measurements should be repeated until

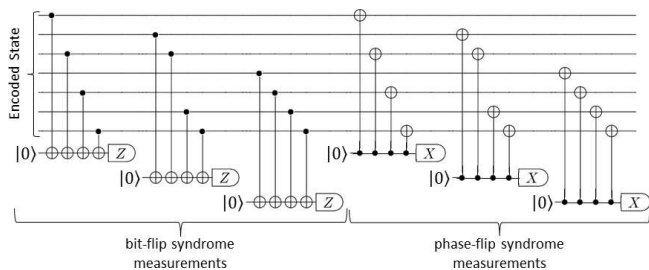


FIG. 1: Non-fault tolerant circuit for syndrome measurements for the  $[[7,1,3]]$  QEC code using single qubit ancilla.

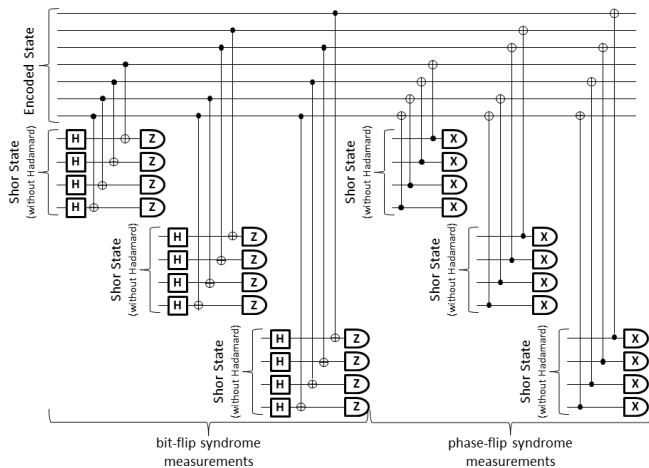


FIG. 2: Fault tolerant circuit for syndrome measurements for the  $[[7,1,3]]$  QEC code using Shor states. To ensure fault tolerance each set of bit-flip and phase-flip syndromes is repeated until the same syndrome is read out twice in a row.

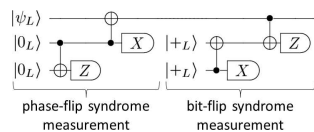


FIG. 3: Fault tolerant circuit for syndrome measurements for the  $[[7,1,3]]$  QEC code using Steane ancilla. Each line represents seven physical qubits. The circuit shows that each ancilla is verified to check for errors that may have occurred during non-fault tolerant construction.

the same syndrome is read out twice.

A second method of performing  $[[7,1,3]]$  code syndrome measurements in a fault tolerant fashion is via the use of Steane ancilla [4] as shown in Fig. 3. A Steane ancilla is a seven qubit system in the logical  $|0\rangle$  or  $|+\rangle$  state of the  $[[7,1,3]]$  QEC code for phase-flip and bit-flip syndrome measurements, respectively. To identify a bit- (phase-) flip error a logical controlled-NOT (CNOT) gate is applied between the data qubits and ancilla qubits with the data qubits (ancilla qubits) as the control. The ancilla qubits are measured to determine the syndrome. To construct the ancilla in a fault tolerant fashion, two copies of the logical  $|0\rangle$  or  $|+\rangle$  state are made following the non-fault tolerant gate sequence of Ref. [4]. A logical CNOT gate is applied between the two copies and one is measured to check for possible construction errors in the other. Unlike the Shor state method, syndrome measurement using Steane states need only be applied once per QEC application to fulfill the requirements of QFT [8]. Nevertheless, we will find that, at times, better results will emerge if we apply the syndrome measurements twice per QEC application.

In this paper we explore  $[[7,1,3]]$  QEC code error correction with each of these syndrome measurement methods by simulating the implementation of 50 gates on a logical qubit in different error environments. For each

syndrome measurement method we implement QEC after different numbers of gates to determine how often it is best to apply QEC. We then compare the fidelity of the three syndrome measurement methods.

Within the QFT framework the only proper gate operations are those which will keep quantum information protected at all times and are designed in such a way as to stem any possible spread of errors. An appropriate choice of universal gate set for many QEC codes, including the  $[[7,1,3]]$  code, are Clifford gates plus the  $T$ -gate, a single-qubit  $\pi/4$  phase rotation. For Calderbank-Shor-Steane (CSS) codes, Clifford gates can be implemented bit-wise while the  $T$ -gate requires a specially prepared ancilla state and a series of controlled-NOT gates. Such a restrictive gate set means that many gates must be applied to accomplish what may superficially appear to be a straightforward task. For example, much work has been done to determine optimal gate sequences for implementing an arbitrary single-qubit rotation (within prescribed accuracy  $\epsilon$ ) using only the gates Clifford plus  $T$ . [9–17]. The goal of these works has been to find as short a gate sequence as possible with the fewest number of resource-consuming  $T$ -gates. Recent results allow, for example, a  $\sigma_z$  rotation by 0.1 to be implemented within an accuracy of  $10^{-5}$  by using 56 [17]  $T$ -gates, interspersed by one or two Hadamard,  $H$ , and Phase,  $P$ , gates. Thus, a fault tolerant implementation of this rotation would require more than 100 gates. Applying QEC after each gate, as is assumed for fault tolerant quantum computation, thus costs thousands of qubits and hundreds of time steps just to implement a single rotation.

## II. SIMULATION MODEL

Recent work has begun to analyze different approaches to the implementation of various quantum computing protocols with the goal of optimizing fidelity and resource consumption [18–22, 30]. Specifically, the suggestion of applying QEC less often so as to save valuable resources has been explored in [23–25]. These works show that applying QEC after every gate will not necessarily optimize the accuracy of the algorithm being implemented. Here, we extend previous work by exploring multiple syndrome measurement methods.

Every step of our simulations, except for the initial state encoding, is performed in a nonequiprobable Pauli operator error environment [26] with non-correlated errors. As in [27], this error model is a stochastic version of a biased noise model that can be formulated in terms of Hamiltonians coupling the system to an environment. In our simulations different error types arise with different probabilities. Individual qubits undergo  $\sigma_x^j$  errors with probability  $p_x$ ,  $\sigma_y^j$  errors with probability  $p_y$ , and  $\sigma_z^j$  errors with probability  $p_z$ , where  $\sigma_i^j$ ,  $i = x, y, z$  are the Pauli spin operators on qubit  $j$ . Only qubits taking part in a gate operation, initialization, or measurement will be subject to error while other qubits are perfectly stored.

Qubits taking part in a two-qubit gate will undergo errors independently. The idealized assumption that idle qubits are not subject to error is partially justified in that it is expected such qubits will be less likely to undergo error (see for example [28]).

We assume a single qubit state  $|\psi\rangle = \cos\alpha|0\rangle + e^{i\beta}\sin\alpha|1\rangle$ , perfectly encoded into the  $[[7,1,3]]$  error correction code. A series of (necessarily noisy) logical gates,  $U_{50}\dots U_2U_1$ , is implemented in the nonequiprobable error environment with (noisy) error correction applied at varying intervals leading to a final state,  $\rho_f$ , of the 7 qubits. To determine the accuracy of the simulated implementations with perfectly applied gates,  $\rho_i$ , we utilize the state fidelity  $F(\rho_i, \rho_f) = \text{Tr}[\rho_i\rho_f]$ . In addition we will find it useful to utilize the infidelity  $I(\rho_i, \rho_f) = 1 - F(\rho_i, \rho_f)$ .

The composite gates  $A = HPT$  and  $B = HT$  are basic building blocks for gate sequences that implement arbitrary single qubit rotations from the gate set Clifford plus  $T$ . For our simulations we implement 20 randomly chosen composite gates (comprising 50 total gates):

$$U = ABBBAAAABBABABBBBAA, \quad (1)$$

with all gates and associated ancilla construction implemented in the non-equiprobable error environment. We simulate 7 QEC application schemes: applying QEC after every gate, ( $q = 50$ , where  $q$  is the number of QEC applications), after every composite gate  $A$  and  $B$  ( $q = 20$ ), after every two composite gates ( $q = 10$ ), after every five composite gates ( $q = 4$ ), after each half of the sequence  $U$  ( $q = 2$ ), after the entire sequence ( $q = 1$ ), and not applying QEC at all ( $q = 0$ ). Every physical gate of the QEC implementation, including syndrome measurement construction, is done in the nonequiprobable error environment. Each scheme is simulated for error environments of different values of  $p_x$ ,  $p_y$  and  $p_z$ . Our initial state is the basis state  $|0\rangle$ . Other initial states and gate sequences were explored and give similar results.

To implement a logical Clifford gate,  $C$ , within the  $[[7,1,3]]$  QEC code one implements the gate  $C^\dagger$  on each of the 7 physical qubits. To implement a logical  $T$ -gate on the  $[[7,1,3]]$  QEC code requires constructing the ancilla state  $|\Theta\rangle = \frac{1}{\sqrt{2}}(|0_L\rangle + e^{i\frac{\pi}{4}}|1_L\rangle)$ , where  $|0_L\rangle$  and  $|1_L\rangle$  are the logical basis states of the  $[[7,1,3]]$  QEC code. Bit-wise CNOT gates are then applied between the state  $|\Theta\rangle$  and the encoded state with the  $|\Theta\rangle$  state qubits as control. A measurement outcome of zero on the encoded state projects the qubits of the  $|\Theta\rangle$  state into the state  $T$  acting on the encoded state. Our simulations are done in a fault tolerant fashion following [20] and every step is done in the nonequiprobable error environment.

Simulations were performed for four error environments: depolarization,  $p = p_x = p_y = p_z$ , and when one of the error probabilities,  $p_i$  is dominant and the other two  $p_j = p_k = 10^{-10}$ . Results for the Shor state syndrome measurement method were reported in [24]. Here we recall those results, report on results for the other two syndrome measurement methods, and compare and

TABLE I: Second line: infidelity of final state after 50 noisy gates with noisy QEC using Shor states for syndrome measurements applied after each gate as a function of depolarization strength  $p$ . Lower lines: fractional change of infidelity,  $D(I_{50}, I_q)$ , for different QEC application schemes.

q	$p = 10^{-6}$	$p = 10^{-5}$	$p = 10^{-4}$	$p = 10^{-3}$
50	$4.50 \times 10^{-5}$	$4.54 \times 10^{-4}$	$4.90 \times 10^{-3}$	$8.27 \times 10^{-2}$
20	$7.54 \times 10^{-6}$	$7.55 \times 10^{-5}$	$7.62 \times 10^{-4}$	$7.85 \times 10^{-3}$
10	$2.76 \times 10^{-6}$	$2.80 \times 10^{-5}$	$3.13 \times 10^{-4}$	$4.97 \times 10^{-3}$
4	$-1.94 \times 10^{-6}$	$-1.89 \times 10^{-5}$	$-1.39 \times 10^{-4}$	$1.52 \times 10^{-3}$
2	$-2.71 \times 10^{-6}$	$-2.65 \times 10^{-5}$	$-2.12 \times 10^{-4}$	$9.88 \times 10^{-4}$
1	$-3.38 \times 10^{-6}$	$-3.31 \times 10^{-5}$	$-2.76 \times 10^{-4}$	$5.12 \times 10^{-4}$
0	-1.02	-1.01	-.941	-.544

contrast the results of the three syndrome measurement methods.

We present our results via a series of Tables augmented by Figures found in the Appendix which will allow us to determine the optimum syndrome measurement method as a function of both fidelity and resources consumed. Each table looks at a single syndrome measurement method and compares the fidelity of the output state after 50 gates for the different values of  $q$ , the number of times QEC is applied. The first line in each Table shows the error probability  $p_i$ . The second line gives the infidelity of the output state after the 50 gates when QEC is applied after every gate,  $I_{50}$ . The remaining lines show the fractional change,  $D$ , of the infidelity when using the other QEC application schemes:

$$D(I_{50}, I_q) = \frac{I_{50} - I_q}{I_{50}} \quad (2)$$

for  $q = 20, 10, 4, 2, 1, 0$ . A positive fractional change means a higher fidelity when using less QEC. Negative fractional change means the fidelity is higher when applying QEC after every gate. However, it is important to note applying QEC after every gate is the most resource intensive. Thus, even if it gives the highest fidelity, it may not be the optimal choice of QEC application schemes.

### III. DEPOLARIZATION ENVIRONMENT

Our first set of tables look at the infidelity of the output states after application of 50 gates and  $q$  QEC applications in a depolarizing environment. The five tables correspond to five different syndrome measurement methods: the Shor state method, during which syndrome measurements are applied twice per QEC application, the Steane method, during which the syndrome measurements are implemented once and twice per QEC application, and the single qubit ancilla method, where the syndrome measurements are implemented once and twice per QEC application.

When implementing QEC with Shor states in a depolarizing environment the best strategy for extremely low

TABLE II: Second line: infidelity of final state after 50 noisy gates with noisy QEC using single ancilla qubits for syndrome measurements applied after each gate as a function of depolarization strength  $p = p_x = p_y = p_z$ . Each QEC application consists of one set of syndrome measurements. Lower lines: fractional change of infidelity,  $D(I_{50}, I_q)$ , for different QEC application schemes.

q	$p = 10^{-6}$	$p = 10^{-5}$	$p = 10^{-4}$	$p = 10^{-3}$
50	$4.20 \times 10^{-5}$	$4.24 \times 10^{-4}$	$4.62 \times 10^{-3}$	$8.08 \times 10^{-2}$
20	$1.53 \times 10^{-5}$	$1.51 \times 10^{-4}$	$1.39 \times 10^{-3}$	$7.41 \times 10^{-3}$
10	$-8.92 \times 10^{-6}$	$-8.84 \times 10^{-5}$	$-8.11 \times 10^{-4}$	$-4.49 \times 10^{-3}$
4	$-3.29 \times 10^{-5}$	$-3.27 \times 10^{-4}$	$-3.01 \times 10^{-3}$	$-1.67 \times 10^{-2}$
2	$-3.67 \times 10^{-5}$	$-3.64 \times 10^{-4}$	$-3.35 \times 10^{-3}$	$-1.88 \times 10^{-2}$
1	$-4.00 \times 10^{-5}$	$-3.97 \times 10^{-4}$	$-3.66 \times 10^{-3}$	$-2.06 \times 10^{-2}$
0	-1.17	-1.15	-1.06	-.578

TABLE III: Second line: infidelity of final state after 50 noisy gates with noisy QEC using single ancilla qubits for syndrome measurements applied after each gate as a function of depolarization strength  $p = p_x = p_y = p_z$ . Each QEC application consists of two sets of syndrome measurements. Lower lines: fractional change of infidelity,  $D(I_{50}, I_q)$ , for different QEC application schemes.

q	$p = 10^{-6}$	$p = 10^{-5}$	$p = 10^{-4}$	$p = 10^{-3}$
50	$4.20 \times 10^{-5}$	$4.24 \times 10^{-4}$	$4.60 \times 10^{-3}$	$7.92 \times 10^{-2}$
20	$2.70 \times 10^{-5}$	$2.68 \times 10^{-4}$	$2.48 \times 10^{-3}$	$1.38 \times 10^{-2}$
10	$2.98 \times 10^{-5}$	$2.95 \times 10^{-4}$	$2.73 \times 10^{-3}$	$1.48 \times 10^{-2}$
4	$3.06 \times 10^{-5}$	$3.04 \times 10^{-4}$	$2.79 \times 10^{-3}$	$1.46 \times 10^{-2}$
2	$3.12 \times 10^{-5}$	$3.09 \times 10^{-4}$	$2.84 \times 10^{-3}$	$1.47 \times 10^{-2}$
1	$3.15 \times 10^{-5}$	$3.12 \times 10^{-4}$	$2.86 \times 10^{-3}$	$1.47 \times 10^{-2}$
0	-1.17	-1.16	-1.07	-.611

values of  $p$  is to apply QEC after every gate (not shown). This is hardly surprising since, at these low error probabilities, the cost of fidelity in applying QEC is minimal. As  $p$  increases the optimal choice of QEC application scheme will be the one that best balances errors arising during gate implementation and errors arising from the QEC application. Table I shows that two QEC schemes  $q = 10, 20$  yield a higher fidelity than QEC after every gate. For  $p \geq 10^{-3}$  applying QEC after every gate gives the lowest fidelity because the high fidelity cost of applying QEC outweighs the gain in correcting gate implementation errors.

The one qubit syndrome ancilla is a non-fault tolerant syndrome measurement method. Nevertheless, we see that the fidelity of the output state after 50 gates applying QEC with this syndrome measurement is actually higher than the fidelity when QEC is implemented with Shor states. We look at two variations of this syndrome measurement scheme: applying the syndrome measurements once per QEC application and twice per QEC application. While the fidelity when applying QEC after every gate is practically the same with both methods, we see that different QEC applications schemes lead to different results.

TABLE IV: Second line: infidelity of final state after 50 noisy gates with noisy QEC using Steane state syndrome measurements applied after each gate as a function of depolarization strength  $p = p_x = p_y = p_z$ . Each QEC application consists of one set of syndrome measurements. Lower lines: fractional change of infidelity,  $D(I_{50}, I_q)$ , for different QEC application schemes.

q	$p = 10^{-6}$	$p = 10^{-5}$	$p = 10^{-4}$	$p = 10^{-3}$
50	$3.50 \times 10^{-5}$	$3.55 \times 10^{-4}$	$3.96 \times 10^{-3}$	$7.84 \times 10^{-2}$
20	$-1.74 \times 10^{-4}$	$-1.72 \times 10^{-3}$	$-1.55 \times 10^{-2}$	$-7.65 \times 10^{-2}$
10	$-1.78 \times 10^{-4}$	$-1.76 \times 10^{-3}$	$-1.58 \times 10^{-2}$	$-7.76 \times 10^{-2}$
4	$-2.15 \times 10^{-4}$	$-2.12 \times 10^{-3}$	$-1.91 \times 10^{-2}$	$-9.36 \times 10^{-2}$
2	$-2.14 \times 10^{-4}$	$-2.12 \times 10^{-3}$	$1.91 \times 10^{-2}$	$-9.37 \times 10^{-2}$
1	$-2.17 \times 10^{-4}$	$-2.15 \times 10^{-3}$	$-1.93 \times 10^{-2}$	$-9.50 \times 10^{-2}$
0	-1.60	-1.58	-1.40	-.628

When the syndrome measurements are applied once per QEC application we find that the best QEC scheme is  $q = 20$  followed by applying QEC after every gate as shown in Table II. In contrast, when syndrome measurements are applied twice per QEC application we find that in general the less QEC is applied the better (as long as it is applied), as shown in Table III. For error probabilities  $10^{-10} \leq p \leq 10^{-2}$  applying QEC after every gate always gives the worst fidelity and applying QEC once is generally the best. Only on the edges of this range,  $p = 10^{-2.5}$  and  $10^{-9.5}$ , do we find that the best QEC scheme is  $q = 10$ . For  $p = 10^{-2}$  things turn around and applying QEC more often is better and thus applying QEC after every gate gives the highest fidelity. A comparison of the fidelities of the best QEC application schemes for the two single-qubit syndrome measurement variations is shown in the top-left inset of Fig. 4. While on the the scale of the plot the fidelities are extremely close, the figure highlights that the best scheme for QEC when syndrome measurements are applied once  $q = 20$  and when syndrome measurements are applied twice it is  $q = 1$ . Thus, applying syndrome measurements twice per QEC leadsto a factor of 10 savings in time and resources and, in addition, the fidelity of this scheme is slightly higher.

Using Steane states for syndrome measurements gives the highest fidelity amongst the syndrome measurement methods explored here. If each QEC consists of one application of the syndrome measurements (which is still fault tolerant) than the best scheme is to apply QEC after every gate as shown in Table IV. If each QEC encompasses two such applications  $q = 10$  is the best scheme and ordering of the other schemes depends on  $p$  as shown in Table V. A comparison of the fidelities of the best QEC application schemes for the two Steane state syndrome measurement variations is shown in the bottom-right inset of Fig. 4. While on the the scale of the plot the fidelities are extremely close, the figure highlights that the best scheme for QEC when syndrome measurements are applied once is generally  $q = 50$  and when syndrome measurements are applied twice it is generally

TABLE V: Second line: infidelity of final state after 50 noisy gates with noisy QEC using Steane state syndrome measurements applied after each gate as a function of depolarization strength  $p = p_x = p_y = p_z$ . Each QEC application consists of two sets of syndrome measurements. Lower lines: fractional change of infidelity,  $D(I_{50}, I_q)$ , for different QEC application schemes.

q	$p = 10^{-6}$	$p = 10^{-5}$	$p = 10^{-4}$	$p = 10^{-3}$
50	$3.50 \times 10^{-5}$	$3.54 \times 10^{-4}$	$3.91 \times 10^{-3}$	$7.35 \times 10^{-2}$
20	$-2.77 \times 10^{-6}$	$-2.77 \times 10^{-5}$	$-2.76 \times 10^{-4}$	$-2.68 \times 10^{-3}$
10	$5.35 \times 10^{-6}$	$5.27 \times 10^{-5}$	$4.53 \times 10^{-4}$	$9.64 \times 10^{-4}$
4	$3.69 \times 10^{-7}$	$3.27 \times 10^{-6}$	$-5.10 \times 10^{-6}$	$-1.83 \times 10^{-3}$
2	$2.56 \times 10^{-6}$	$2.49 \times 10^{-5}$	$1.91 \times 10^{-4}$	$-9.11 \times 10^{-4}$
1	$3.05 \times 10^{-6}$	$2.98 \times 10^{-5}$	$2.34 \times 10^{-4}$	$-7.62 \times 10^{-4}$
0	-1.60	-1.58	-1.43	-0.735

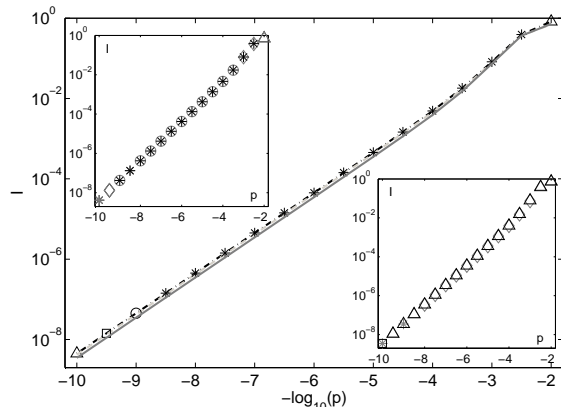


FIG. 4: Infidelity versus error probability comparison of three syndrome measurement methods: Shor state (black, chain), single qubit with syndrome measurements twice per QEC (light gray, dashed), and Steane state with syndrome measurements twice per QEC (gray, solid). The markers show which Shor state QEC application scheme gives the best fidelity for the corresponding  $p$ :  $q = 50$  ( $\triangle$ ),  $q = 20$  ( $*$ ),  $q = 10$  ( $\diamond$ ),  $q = 4$  ( $\square$ ),  $q = 2$  ( $\times$ ), and  $q = 1$  ( $\circ$ ). The insets compare the difference between applying syndrome measurements once per QEC application (dark markers) versus twice per QEC application (light markers) for the one-qubit syndrome measurements (upper left) and Steane state (lower right) syndrome measurements.

$q = 10$ . Thus, applying syndrome measurements twice per QEC leads to a factor of 2.5 savings in time and resources and, in addition, the fidelity of this scheme is slightly better.

Figure 4 compares the infidelity of the best of each of the three syndrome measurement methods. Clearly using Steane states for syndrome measurements gives the highest fidelity. It should be noted, however, that the three fidelities are not that different and the single-qubit syndrome measurements give a comparable fidelity (and one better than the Shor state syndrome measurements) despite the fact that it is not fault tolerant.

#### IV. ASYMMETRIC ERROR ENVIRONMENTS

The next set of five tables look at the infidelity of the output states after simulation of 50 logical gates and  $q$  QEC applications in error environments where one of the error probabilities  $p_i$  is dominant and the other error probabilities  $p_j, p_k$  are equal to  $10^{-10}$ .

The asymmetric error environment demonstrates the effectiveness of tailoring QEC to the particular evolution of the system. We first look at using Shor states for syndrome measurements in Table VI. When  $\sigma_y$  errors are dominant applying QEC after each gate is always optimal unless  $p_y \geq 10^{-5.5}$  in which case  $q = 20$  gives higher fidelity. When phase-flip errors are dominant, applying QEC after every gate gives the worst fidelity (besides not applying QEC at all). The other schemes are about equal but the best fidelity is achieved for  $q = 4$ . When bit-flip errors are dominant not applying QEC at all leads to the highest fidelity by far [24, 30].

For syndrome measurements done via a one-qubit ancilla we also see a strong dependence on the error environment. If each application of QEC consists of one set of syndrome measurements Table VII demonstrates that  $q = 20$  gives the best fidelity when bit-flip errors are dominant,  $q = 50$  gives the best fidelity when  $\sigma_y$  errors are dominant, and  $q = 4$  gives the best fidelity when phase-flip errors are dominant.

When each QEC application consists of two sets of syndrome measurements the situation changes as shown in Table VII. When bit-flip errors are dominant it is best to apply QEC only after all 50 gates,  $q = 1$ . When  $\sigma_y$  errors dominate  $q = 50$  gives the best fidelity for error probabilities between  $10^{-9}$  and  $10^{-6}$ . For higher error probabilities, the  $q = 20$  gives the highest fidelity. When phase-flip errors are dominant,  $q = 1$  again gives the highest fidelity.

A comparison of the fidelities of the best QEC application schemes for the two single-qubit syndrome measurement variations in the different error environments is shown in the top-left insets of Fig. 5. For a bit-flip dominated environment when  $10^{-8} < p_x < 10^{-4}$  the fidelity is lightly higher when syndrome measurements are applied once per QEC than when applied twice per QEC. Furthermore, QEC in the former case should be applied two-and-a-half times less leading to resource saving by a factor of 5. When  $\sigma_y$  errors are dominant we find that applying the syndrome measurement set twice per QEC generally gives better fidelity and also gives a slight advantage in resources. When phase-flip errors dominate applying syndrome measurements twice per QEC gives a slightly higher fidelity and uses only half the resources since QEC can be applied only once.

When using Steane states for syndrome measurements we again see different behavior. When each QEC consists of one syndrome measurement there is a sharp distinction between whether bit-flip or phase-flip errors are dominant. Table X shows that when bit-flip errors dominate applying QEC after every gate is optimal. When

TABLE VI: Second line: infidelity of final state after 50 noisy gates with noisy QEC using Shor states for syndrome measurements applied after each gate as a function of  $p_i$  with  $p_j = p_k = 10^{-10}$ . Lower lines: fractional change of infidelity,  $D(I_{50}, I_q)$ , for different QEC application schemes.

q	$p_x = 10^{-7}$	$p_x = 10^{-5}$	$p_x = 10^{-3}$	$p_y = 10^{-7}$	$p_y = 10^{-5}$	$p_y = 10^{-3}$	$p_z = 10^{-7}$	$p_z = 10^{-5}$	$p_z = 10^{-3}$
50	$3.1 \times 10^{-6}$	$3.1 \times 10^{-4}$	$3.2 \times 10^{-2}$	$7.0 \times 10^{-7}$	$7.0 \times 10^{-5}$	$1.1 \times 10^{-2}$	$7.0 \times 10^{-7}$	$7.1 \times 10^{-5}$	$1.9 \times 10^{-2}$
20	$2.9 \times 10^{-10}$	$1.6 \times 10^{-7}$	$1.5 \times 10^{-3}$	$-1.6 \times 10^{-10}$	$6.7 \times 10^{-9}$	$7.2 \times 10^{-5}$	$3.9 \times 10^{-6}$	$3.8 \times 10^{-4}$	$1.8 \times 10^{-2}$
10	$1.4 \times 10^{-10}$	$2.0 \times 10^{-7}$	$1.9 \times 10^{-3}$	$-2.2 \times 10^{-9}$	$-3.7 \times 10^{-8}$	$-2.0 \times 10^{-4}$	$3.9 \times 10^{-6}$	$3.8 \times 10^{-4}$	$1.9 \times 10^{-2}$
4	$4.7 \times 10^{-10}$	$2.4 \times 10^{-7}$	$2.4 \times 10^{-3}$	$-2.1 \times 10^{-9}$	$-1.1 \times 10^{-7}$	$-6.3 \times 10^{-4}$	$4.0 \times 10^{-6}$	$4.0 \times 10^{-4}$	$1.9 \times 10^{-2}$
2	$3.9 \times 10^{-10}$	$2.4 \times 10^{-7}$	$2.4 \times 10^{-3}$	$-3.5 \times 10^{-9}$	$-1.1 \times 10^{-7}$	$-6.9 \times 10^{-4}$	$3.9 \times 10^{-6}$	$3.8 \times 10^{-4}$	$1.9 \times 10^{-2}$
1	$4.3 \times 10^{-10}$	$2.5 \times 10^{-7}$	$2.4 \times 10^{-3}$	$-5.0 \times 10^{-9}$	$-1.2 \times 10^{-7}$	$-7.6 \times 10^{-4}$	$3.8 \times 10^{-6}$	$3.8 \times 10^{-4}$	$1.9 \times 10^{-2}$
0	$9.5 \times 10^{-2}$	$9.6 \times 10^{-2}$	$8.1 \times 10^{-2}$	-2.0	-2.0	-1.3	-5.0	-4.9	-1.8

TABLE VII: Second line: infidelity of final state after 50 noisy gates with noisy QEC using single ancilla qubits for syndrome measurements applied after each gate as a function of  $p_i$  with  $p_j = p_k = 10^{-10}$ . Each QEC application consists of one set of syndrome measurements. Lower lines: fractional change of infidelity,  $D(I_{50}, I_q)$ , for different QEC application schemes.

q	$p_x = 10^{-7}$	$p_x = 10^{-5}$	$p_x = 10^{-3}$	$p_y = 10^{-7}$	$p_y = 10^{-5}$	$p_y = 10^{-3}$	$p_z = 10^{-7}$	$p_z = 10^{-5}$	$p_z = 10^{-3}$
50	$2.8 \times 10^{-6}$	$2.8 \times 10^{-4}$	$2.9 \times 10^{-2}$	$7.0 \times 10^{-7}$	$7.0 \times 10^{-5}$	$1.1 \times 10^{-2}$	$7.0 \times 10^{-7}$	$7.1 \times 10^{-5}$	$2.0 \times 10^{-2}$
20	$2.7 \times 10^{-7}$	$2.7 \times 10^{-5}$	$2.7 \times 10^{-3}$	$-8.1 \times 10^{-7}$	$-8.1 \times 10^{-5}$	$-5.4 \times 10^{-3}$	$1.1 \times 10^{-5}$	$1.1 \times 10^{-3}$	$4.1 \times 10^{-2}$
10	$6.0 \times 10^{-8}$	$6.4 \times 10^{-6}$	$7.2 \times 10^{-4}$	$-2.4 \times 10^{-6}$	$-2.4 \times 10^{-4}$	$-1.6 \times 10^{-2}$	$1.3 \times 10^{-5}$	$1.2 \times 10^{-3}$	$4.5 \times 10^{-2}$
4	$8.3 \times 10^{-8}$	$8.8 \times 10^{-6}$	$1.1 \times 10^{-3}$	$-4.2 \times 10^{-6}$	$-4.3 \times 10^{-4}$	$-2.9 \times 10^{-2}$	$1.3 \times 10^{-5}$	$1.2 \times 10^{-3}$	$4.7 \times 10^{-2}$
2	$4.9 \times 10^{-8}$	$5.2 \times 10^{-6}$	$7.1 \times 10^{-4}$	$-4.6 \times 10^{-6}$	$-4.6 \times 10^{-4}$	$-3.1 \times 10^{-2}$	$1.3 \times 10^{-5}$	$1.3 \times 10^{-3}$	$4.7 \times 10^{-2}$
1	$3.5 \times 10^{-8}$	$4.1 \times 10^{-6}$	$5.7 \times 10^{-4}$	$-4.9 \times 10^{-6}$	$-4.8 \times 10^{-4}$	$-3.2 \times 10^{-2}$	$1.3 \times 10^{-5}$	$1.3 \times 10^{-3}$	$4.7 \times 10^{-2}$
0	$-1.8 \times 10^{-3}$	$-1.2 \times 10^{-4}$	$-1.0 \times 10^{-2}$	-2.0	-2.0	-1.3	-5.0	-4.9	-1.6

phase-flip errors dominate applying QEC after all the gates is optimal. For  $\sigma_y$  errors only  $q = 20$  gives better fidelity than applying QEC after every gate. When each QEC application consists of two sets of syndrome measurements it is best to apply QEC only once,  $q = 1$ , if  $\sigma_y$  or phase-flips are the dominant error. If bit-flips are dominant the best QEC method depends on the strength of  $p_x$ . If  $p_x > 10^{-5.5}$  the best method is  $q = 4$ . For weaker  $p_x$  the best method is either  $q = 50$  or  $q = 20$  depending on the exact error strength.

A comparison of the fidelities of the best QEC application schemes for the two Steane state syndrome measurement variations in the different error environments is shown in the bottom-right insets of Fig. 5. For a bit-flip dominated environment the fidelity is higher when syndrome measurements are applied twice per QEC, though this sometimes comes with a cost in the amount of resources used. When  $\sigma_y$  errors dominate applying syndrome measurements twice gives a slightly higher fidelity and will also provide up to a factor of 10 in resource savings over applying the syndrome measurements just once. When phase-flip errors dominate applying syndrome measurements twice per QEC gives a slightly higher fidelity than applying just once per QEC. However, this increase in fidelity comes at a cost of using two times the resources.

Figure 5 compares the infidelity of the best of each of the three syndrome measurement methods in asymmetric error environments. For the bit-flip and  $\sigma_y$  error dominated environments the Steane state ancilla give the best fidelity, by a wide margin for bit-flips and by only a slight

margin for  $\sigma_y$  errors. In a phase-flip dominated environment the Steane syndrome measurements give the lowest fidelity. In all three error environments the fidelity of the Shor state syndromes and that of the single-qubit syndromes are similar, though the single qubit syndromes give a slightly better fidelity.

## V. CONCLUSION

In conclusion we have explored different syndrome measurement techniques for the  $[[7,1,3]]$  QEC code in different error environments. The three syndrome measurements explored are those using Shor states and Steane states, each of which are fault tolerant, and using a single qubit ancilla, which is not fault tolerant. We explore two variations of both the Steane state and single-qubit syndrome measurement methods: the syndrome measurements are applied once per QEC application and twice per QEC application. The simulations implement 50 logical gates within the  $[[7,1,3]]$  QEC encoding with QEC applied at various intervals using the different types of syndrome measurements. The results demonstrate that the optimal syndrome measurements to use will strongly depend on the error environment. In a depolarizing environment and when bit-flip and  $\sigma_y$  errors dominate, the best syndrome measurements to use are the Steane states. When phase-flip errors are dominant we see that the Steane state syndrome measurements give the lowest fidelity. The Shor state and single-qubit syndrome measurements always give similar fidelities with

TABLE VIII: Second line: infidelity of final state after 50 noisy gates with noisy QEC using single ancilla qubits for syndrome measurements applied after each gate as a function of  $p_i$  with  $p_j = p_k = 10^{-10}$ . Each QEC application consists of two sets of syndrome measurements. Lower lines: fractional change of infidelity,  $D(I_{50}, I_q)$ , for different QEC application schemes.

q	$p_x = 10^{-7}$	$p_x = 10^{-5}$	$p_x = 10^{-3}$	$p_y = 10^{-7}$	$p_y = 10^{-5}$	$p_y = 10^{-3}$	$p_z = 10^{-7}$	$p_z = 10^{-5}$	$p_z = 10^{-3}$
50	$2.8 \times 10^{-6}$	$2.8 \times 10^{-4}$	$2.9 \times 10^{-2}$	$7.0 \times 10^{-7}$	$7.0 \times 10^{-5}$	$1.1 \times 10^{-2}$	$7.0 \times 10^{-7}$	$7.1 \times 10^{-5}$	$1.9 \times 10^{-2}$
20	$1.3 \times 10^{-6}$	$1.3 \times 10^{-4}$	$1.3 \times 10^{-2}$	$-6.0 \times 10^{-9}$	$1.8 \times 10^{-8}$	$1.2 \times 10^{-4}$	$9.3 \times 10^{-6}$	$9.2 \times 10^{-4}$	$3.5 \times 10^{-2}$
10	$1.7 \times 10^{-6}$	$1.7 \times 10^{-4}$	$1.7 \times 10^{-2}$	$-6.0 \times 10^{-9}$	$1.7 \times 10^{-8}$	$1.1 \times 10^{-4}$	$1.1 \times 10^{-5}$	$1.1 \times 10^{-3}$	$4.3 \times 10^{-2}$
4	$2.3 \times 10^{-6}$	$2.3 \times 10^{-4}$	$2.2 \times 10^{-2}$	$-7.7 \times 10^{-9}$	$9.8 \times 10^{-10}$	$7.9 \times 10^{-6}$	$1.2 \times 10^{-5}$	$1.2 \times 10^{-3}$	$4.6 \times 10^{-2}$
2	$2.3 \times 10^{-6}$	$2.3 \times 10^{-4}$	$2.3 \times 10^{-2}$	$-7.6 \times 10^{-9}$	$-1.6 \times 10^{-9}$	$-1.1 \times 10^{-5}$	$1.2 \times 10^{-5}$	$1.2 \times 10^{-3}$	$4.7 \times 10^{-2}$
1	$2.4 \times 10^{-6}$	$2.4 \times 10^{-4}$	$2.3 \times 10^{-2}$	$-1.0 \times 10^{-8}$	$-4.9 \times 10^{-9}$	$-3.3 \times 10^{-5}$	$1.3 \times 10^{-5}$	$1.3 \times 10^{-3}$	$4.8 \times 10^{-2}$
0	$-1.7 \times 10^{-3}$	$8.6 \times 10^{-6}$	$2.2 \times 10^{-3}$	-2.0	-2.0	-1.3	-5.0	-4.9	-1.8

TABLE IX: Second line: infidelity of final state after 50 noisy gates with noisy QEC using Steane state syndrome measurements applied after each gate as a function of  $p_i$  with  $p_j = p_k = 10^{-10}$ . Each QEC application consists of one set of syndrome measurements. Lower lines: fractional change of infidelity,  $D(I_{50}, I_q)$ , for different QEC application schemes.

q	$p_x = 10^{-7}$	$p_x = 10^{-5}$	$p_x = 10^{-3}$	$p_y = 10^{-7}$	$p_y = 10^{-5}$	$p_y = 10^{-3}$	$p_z = 10^{-7}$	$p_z = 10^{-5}$	$p_z = 10^{-3}$
50	$7.0 \times 10^{-7}$	$7.0 \times 10^{-5}$	$8.1 \times 10^{-3}$	$7.0 \times 10^{-7}$	$7.0 \times 10^{-5}$	$1.1 \times 10^{-2}$	$2.1 \times 10^{-6}$	$2.1 \times 10^{-4}$	$3.7 \times 10^{-2}$
20	$-4.9 \times 10^{-6}$	$-4.9 \times 10^{-4}$	$-4.3 \times 10^{-2}$	$2.8 \times 10^{-7}$	$2.9 \times 10^{-5}$	$1.3 \times 10^{-3}$	$-9.8 \times 10^{-7}$	$-9.5 \times 10^{-5}$	$-4.5 \times 10^{-3}$
10	$-6.8 \times 10^{-6}$	$-6.7 \times 10^{-4}$	$-5.9 \times 10^{-2}$	$-2.5 \times 10^{-6}$	$-2.5 \times 10^{-4}$	$-1.7 \times 10^{-2}$	$5.8 \times 10^{-6}$	$5.8 \times 10^{-4}$	$3.4 \times 10^{-2}$
4	$-7.0 \times 10^{-6}$	$-6.9 \times 10^{-4}$	$-6.1 \times 10^{-2}$	$-6.6 \times 10^{-6}$	$-6.6 \times 10^{-4}$	$-4.4 \times 10^{-2}$	$8.0 \times 10^{-6}$	$8.0 \times 10^{-4}$	$4.5 \times 10^{-2}$
2	$-7.2 \times 10^{-6}$	$-7.1 \times 10^{-4}$	$-6.2 \times 10^{-2}$	$-7.1 \times 10^{-6}$	$-7.0 \times 10^{-4}$	$-4.6 \times 10^{-2}$	$9.0 \times 10^{-6}$	$9.0 \times 10^{-4}$	$5.2 \times 10^{-2}$
1	$-7.2 \times 10^{-6}$	$-7.2 \times 10^{-4}$	$-6.3 \times 10^{-2}$	$-7.6 \times 10^{-6}$	$-7.5 \times 10^{-4}$	$-5.0 \times 10^{-2}$	$9.8 \times 10^{-6}$	$9.8 \times 10^{-4}$	$5.6 \times 10^{-2}$
0	-3.0	-3.0	-2.6	-2.0	-2.0	-1.3	-1.0	-0.99	-0.42

TABLE X: Second line: infidelity of final state after 50 noisy gates with noisy QEC using Steane state syndrome measurements applied after each gate as a function of  $p_i$  with  $p_j = p_k = 10^{-10}$ . Each QEC application consists of one set of syndrome measurements. Lower lines: fractional change of infidelity,  $D(I_{50}, I_q)$ , for different QEC application schemes.

q	$p_x = 10^{-7}$	$p_x = 10^{-5}$	$p_x = 10^{-3}$	$p_y = 10^{-7}$	$p_y = 10^{-5}$	$p_y = 10^{-3}$	$p_z = 10^{-7}$	$p_z = 10^{-5}$	$p_z = 10^{-3}$
50	$7.0 \times 10^{-7}$	$7.0 \times 10^{-5}$	$8.0 \times 10^{-3}$	$7.0 \times 10^{-7}$	$7.0 \times 10^{-5}$	$1.1 \times 10^{-2}$	$2.1 \times 10^{-6}$	$2.1 \times 10^{-4}$	$3.4 \times 10^{-2}$
20	$-1.2 \times 10^{-8}$	$7.8 \times 10^{-8}$	$8.2 \times 10^{-4}$	$3.4 \times 10^{-6}$	$3.4 \times 10^{-4}$	$2.2 \times 10^{-2}$	$2.4 \times 10^{-6}$	$2.4 \times 10^{-4}$	$1.4 \times 10^{-2}$
10	$-1.5 \times 10^{-8}$	$5.6 \times 10^{-8}$	$6.5 \times 10^{-4}$	$4.9 \times 10^{-6}$	$4.9 \times 10^{-4}$	$3.1 \times 10^{-2}$	$5.4 \times 10^{-6}$	$5.3 \times 10^{-4}$	$3.3 \times 10^{-2}$
4	$-1.4 \times 10^{-8}$	$8.2 \times 10^{-8}$	$9.1 \times 10^{-4}$	$5.2 \times 10^{-6}$	$5.2 \times 10^{-4}$	$3.3 \times 10^{-2}$	$6.2 \times 10^{-6}$	$6.2 \times 10^{-4}$	$3.8 \times 10^{-2}$
2	$-1.5 \times 10^{-8}$	$7.6 \times 10^{-8}$	$8.5 \times 10^{-4}$	$5.5 \times 10^{-6}$	$5.5 \times 10^{-4}$	$3.5 \times 10^{-2}$	$6.7 \times 10^{-6}$	$6.7 \times 10^{-4}$	$4.1 \times 10^{-2}$
1	$-1.6 \times 10^{-8}$	$7.5 \times 10^{-8}$	$8.5 \times 10^{-4}$	$5.7 \times 10^{-6}$	$5.7 \times 10^{-4}$	$3.6 \times 10^{-2}$	$7.1 \times 10^{-6}$	$7.0 \times 10^{-4}$	$4.3 \times 10^{-2}$
0	-3.0	-3.0	-2.6	-2.0	-2.0	-1.3	-1.0	-1.0	-0.55

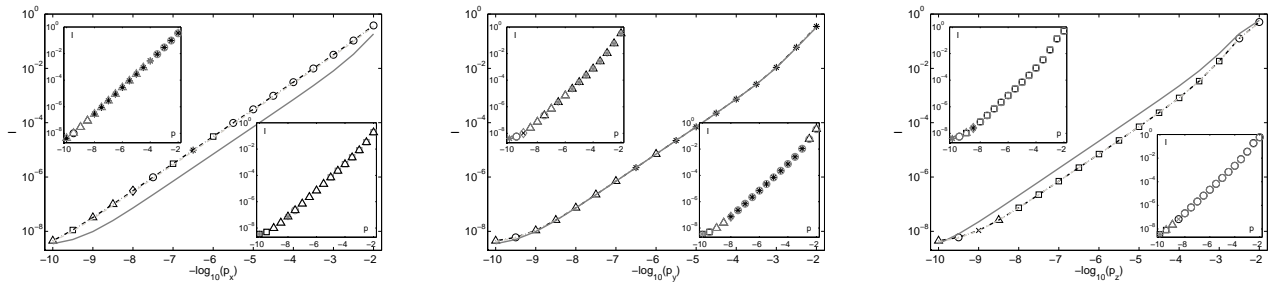


FIG. 5: Infidelity versus error probability comparison of three syndrome measurement methods in asymmetric error models: bit-flip (left),  $\sigma_y$  (right), and phase-flip (left). Shor state (black, chain), single qubit with syndrome measurements twice per QEC (light gray, dashed), and Steane state with syndrome measurements twice per QEC (gray, solid). The markers show which Shor state QEC application scheme gives the best fidelity for the corresponding  $p$ :  $q = 50$  ( $\Delta$ ),  $q = 20$  ( $*$ ),  $q = 10$  ( $\diamond$ ),  $q = 4$  ( $\square$ ),  $q = 2$  ( $\times$ ), and  $q = 1$  ( $\circ$ ). The insets compare the difference between applying syndrome measurements once per QEC application (dark markers) versus twice per QEC application (light markers) for the one-qubit syndrome measurements (upper left) and Steane state (lower right) syndrome measurements.

the single-qubit syndrome measurement fidelity being slightly higher.

In addition, the optimum number of times QEC should be applied within the implementation of the 50 gates also depends on the error environment and the choice of syndrome measurement method. These results allow us to properly weigh resource consumption, time and the number of qubits, versus accuracy as measured via fidelity. Applying QEC only once at the end of 50 gates may save a factor of 50 in resource consumption while sacrificing only a small amount of fidelity.

It is important to note that despite the fact that the single-qubit syndrome measurements are not fault tolerant, they achieve a fidelity that is relatively close to the other syndrome measurements, at least over 50 gates. Whether this condition will hold over larger numbers of gates will be explored elsewhere but it will likely depend strongly on the details of the error environment and how often QEC is applied. Nevertheless, these simulations suggest that perhaps not all the strictures of QFT need be followed to the letter to achieve the desired outcome of a quantum computation.

I would like to thank G. Gilbert for insightful comments. This research is supported under MITRE Innovation Program Grant 51MSR662. ©2014 - The MITRE Corporation. All rights reserved. Approved for Public Release 14-1102; Distribution Unlimited.

## VI. APPENDIX

In this Appendix we provide figures that expand the results shown in Tables by plotting  $D(I_{50}, I_q)/p$  for a range of error probability values. Each of the five figures, one for each syndrome measurement strategy, consists of four subplots, one for each of the four error environment types. Each subplot allows for an easy comparison of the fractional change of the output state after 50 gates compared to applying QEC after every gate for the different values of  $q$ , the number of times QEC is applied. The plots demonstrate which schemes are better (above zero) or worse (below zero) than applying QEC after every gate and by how much.

- 
- [1] M Nielsen and I. Chuang, *Quantum Information and Computation* (Cambridge University Press, Cambridge, 2000).
  - [2] P.W. Shor, Phys. Rev. A **52**, R2493 (1995).
  - [3] A.R. Calderbank and P.W. Shor, Phys. Rev. A **54**, 1098 (1996); A.M. Steane, Phys. Rev. Lett. **77**, 793 (1996).
  - [4] A. Steane, Phys. Rev. Lett. **78**, 2252 (1997).
  - [5] J. Preskill, Proc. Roy. Soc. Lond. A **454**, 385 (1998).
  - [6] P.W. Shor, *Proceedings of the the 35th Annual Symposium on Fundamentals of Computer Science*, (IEEE Press, Los Alamitos, CA, 1996).
  - [7] D. Gottesman, Phys. Rev. A **57**, 127 (1998).
  - [8] P. Aleferis, D. Gottesman, and J. Preskill, Quant. Inf. Comput. **6**, 97 (2006).
  - [9] A.Y. Kitaev, Russ. Math. Surv. **52**, 1191 (1997); A.Y. Kitaev, A.H. Shen, and M.N. Vyalyi, *Classical and Quantum Computation* Graduate Studies in Mathematics **47**, American Mathematical Society 2002.
  - [10] C.M. Dawson and M.A. Nielsen, Quant. Inf. Comp. **6**, 81 (2006).
  - [11] A. Bocharov and K.M. Svore, Phys. Rev. Lett. **109**, 190501 (2012).
  - [12] V. Kliuchnikov, D. Maslov, and M. Mosca, Quant. Inf. Comp. **13**, 607 (2013).
  - [13] T.T. Pham, R. Van Meter, and C. Horsman, arXiv:1209.4139.
  - [14] G. Duclos-Ciani and K.M. Svore, arXiv:1210.1980.
  - [15] V. Kliuchnikov, D. Maslov, and M. Mosca, arXiv:1212.0822.
  - [16] P. Selinger, arXiv:1212.6253.
  - [17] V. Kliuchnikov, D. Maslov, and M. Mosca, arXiv:1212.6964.
  - [18] Y.S. Weinstein, Phys. Rev. A **84**, 012323 (2011).
  - [19] S.D. Buchbinder, C.L. Huang, and Y.S. Weinstein, Quant. Inf. Proc. **12**, 699 (2013).
  - [20] Y.S. Weinstein, Phys. Rev. A **87**, 032320 (2013).
  - [21] A.A. Nanda, B. Fortescue, and M. Byrd, arXiv:1303.4026.
  - [22] Y. Tomita, *et. al*, Phys. Rev. A **88**, 042336 (2013).
  - [23] Y.S. Weinstein, Phys. Rev. A **88**, 012325 (2013).
  - [24] Y.S. Weinstein, Phys. Rev. A **89**, 020301(R) (2014).
  - [25] M.G. Whitney, N. Isailovic, Y. Patel, and J. Kubiawicz, *Proceedings of the 36th Annual International Symposium on Computer Architecture*, (ACM, New York, 2009).
  - [26] V. Aggarwal, A.R. Calderbank, G. Gilbert, Y.S. Weinstein, Quant. Inf. Proc. **9**, 541 (2010).
  - [27] P. Aliferis and J. Preskill, Phys. Rev. A **78**, 052331 (2008).
  - [28] K.M. Svore, B.M. Terhal, D.P. DiVincenzo, Phys. Rev. A **72**, 022317 (2005).
  - [29] I.L. Chuang and M.A. Nielsen J. Mod. Opt. **44**, 2455 (1997).
  - [30] Y.S. Weinstein and S.D. Buchbinder, Phys. Rev. A **86**, 052336 (2012).

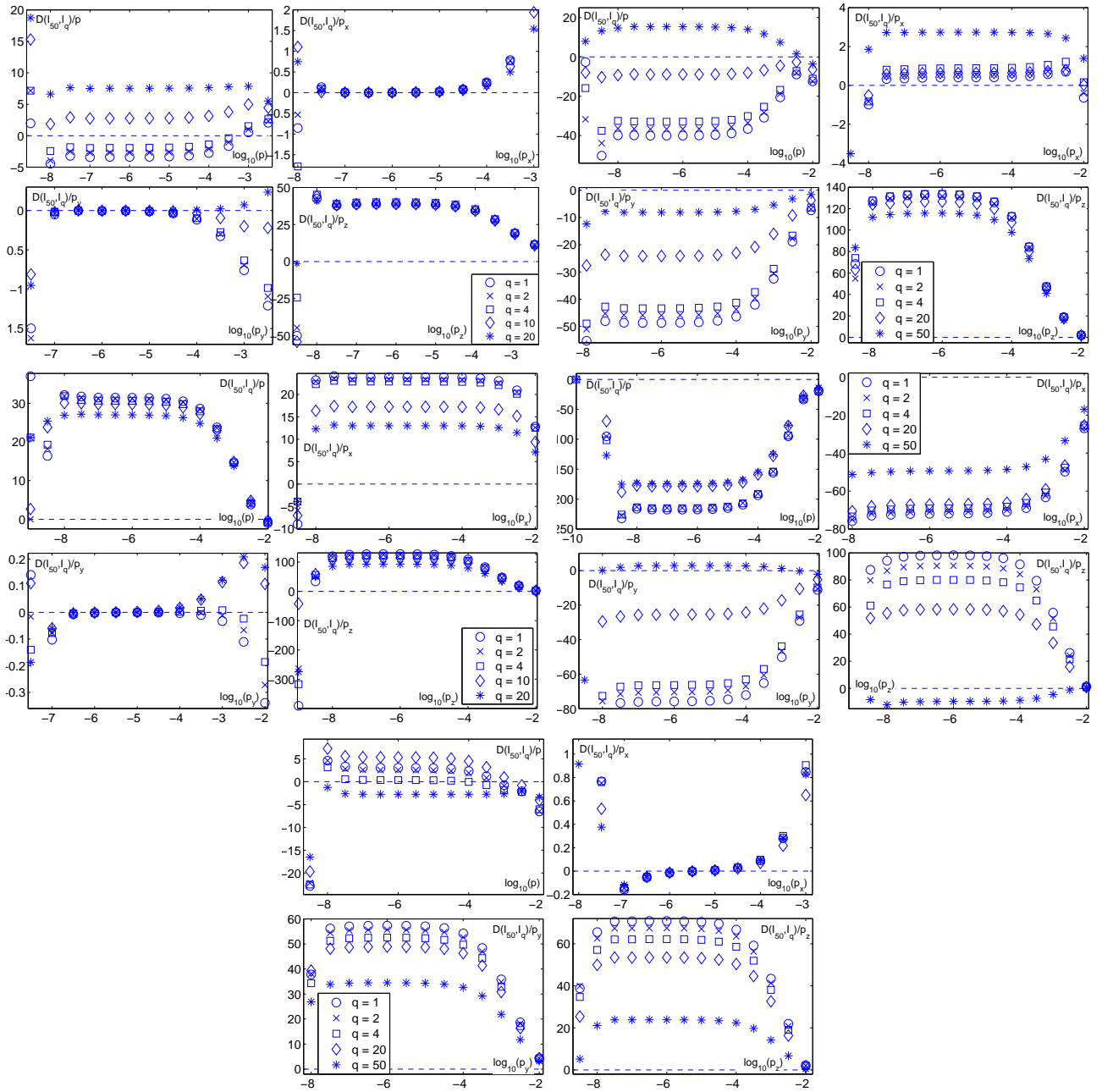


FIG. 6: Fractional change of infidelity of  $\rho_f$  divided by error probability,  $p_i$ , for 50 gates applied to initial state  $|0\rangle$  with  $q = 1$  ( $\circ$ ), 2 ( $\times$ ), 4 ( $\square$ ), 10 ( $\diamond$ ), and 20 ( $*$ ). The subplots are for QEC with Shor states (top left), one-qubit ancilla when each QEC consists of applying syndrome measurements once (top right), one-qubit ancilla when each QEC consists of applying syndrome measurements twice (middle left), Steane states when each QEC consists of applying syndrome measurements once (middle right), and Steane states when each QEC consists of applying syndrome measurements twice (bottom). Within each of the subplots the top left figure is for a depolarizing error environment ( $p = p_x = p_y = p_z$ ) and the remaining figures are for error environments where  $p_i$  is dominant and  $p_j = p_k = 10^{-10}$ :  $i = x$  (top right),  $i = y$  (bottom left) and  $i = z$  (bottom right).